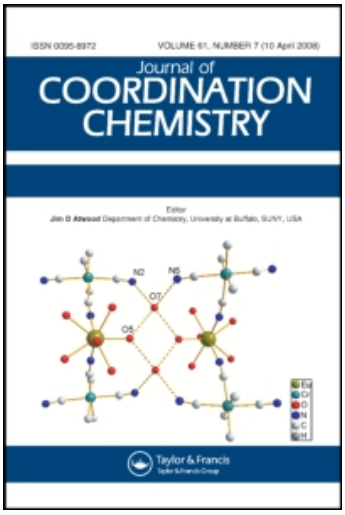

Journal of Coordination Chemistry
Publication details, including instructions for authors and subscription information:
http://www.informaworld.com/smpp/title~content=t713455674

Synthesis, crystal structure, magnetic property, and nuclease activity of a binuclear iron(III) complex

Jing Qian[ab]; Jin-Lei Tian[b]; Li Feng[bc]; Wen Gu[b]; Xiao-Jun Zhao[a]; Shi-Ping Yan[b]
[a] Department of Chemistry, College of Chemistry and Biology, Tianjin Normal University, Tianjin, P.R. China [b] Department of Chemistry, Nankai University, Tianjin, P.R. China [c] Department of Chemistry, Tianjin University of Traditional Chinese Medicine, Tianjin, P.R. China

First published on: 29 July 2010

To cite this Article Qian, Jing , Tian, Jin-Lei , Feng, Li , Gu, Wen , Zhao, Xiao-Jun and Yan, Shi-Ping(2009) 'Synthesis, crystal structure, magnetic property, and nuclease activity of a binuclear iron(III) complex', Journal of Coordination Chemistry, 62: 8, 1260 — 1270, First published on: 29 July 2010 (iFirst)
To link to this Article: DOI: 10.1080/00958970802483632
URL: http://dx.doi.org/10.1080/00958970802483632

Journal of Coordination Chemistry
Vol. 62, No. 8, 20 April 2009, 1260–1270

Taylor & Francis
Taylor & Francis Group

Synthesis, crystal structure, magnetic property, and nuclease activity of a binuclear iron(III) complex

JING QIAN†‡, JIN-LEI TIAN‡, LI FENG‡§, WEN GU‡,
XIAO-JUN ZHAO† and SHI-PING YAN*‡

†Department of Chemistry, College of Chemistry and Biology, Tianjin Normal University, Tianjin, 300387, P.R. China
‡Department of Chemistry, Nankai University, Tianjin, P.R. China
§Department of Chemistry, Tianjin University of Traditional Chinese Medicine, Tianjin, 300193, P.R. China

(*Received 16 January 2008; in final form 23 May 2008*)

A μ-oxo-di-μ-carboxylato-bridged iron(III) complex containing two tridentate nitrogen ligands, $\{[Fe_2(bpma)(bpea)(\mu\text{-}CH_3COO)_2\,\mu\text{-}O)]\cdot(ClO_4)_2\cdot 0.5CH_3OH\}$ (**1**) (bpma = *N*, *N-bis*(2-pyridylmethyl)methyl-amine, bpea = *N*,*N-bis*(2-pyridylmethyl)ethylamine), has been synthesized and determined by X-ray diffraction. Complex **1** crystallizes in the monoclinic space group $P2_1/c$ with $a = 10.9434(12)$ Å, $b = 23.118(3)$ Å, $c = 15.8721(18)$ Å, $\beta = 92.736(2)^\circ$ and $Z = 4$. In **1**, each Fe(III) has a distorted octahedral geometry with a N_3O_3 donor set. The Fe(III) atoms are bridged by two carboxyl groups and one μ-oxo oxygen with Fe1–Fe2 separation of 3.064 Å. Susceptibility data of **1** indicate strong intramolecular antiferromagnetic coupling of the high-spin Fe(III) atoms with $J = -121.0\,cm^{-1}$ and $g = 2.04$. The interaction with calf thymus DNA was investigated by UV absorption and fluorescent spectroscopy. Results show that the complex binds to ct-DNA with a moderate intercalative mode. The interaction between **1** and pBR322 DNA has also been investigated by submarine gel electrophoresis; the complex exhibits effective DNA cleavage activity in the absence of activating agents under similar physiological conditions.

Keywords: Iron(III); Crystal structure; Magnetic property; DNA binding; DNA cleavage

1. Introduction

Transition metal complexes capable of cleaving DNA and RNA under physiological conditions via oxidative and hydrolytic mechanisms are of importance for their potential use as new structural probes in nucleic acid chemistry and as therapeutic agents [1]. Among the active transition metal species, dinuclear, and polynuclear complexes generally give higher cleavage rates provided that the ligand holds the metal centers in an appropriate geometry [2–9]. Compared with mononuclear complexes, dinuclear complexes have higher activity as a result of the cooperative interaction of metal ions in stabilizing the transition state of phosphodiester cleavage. Dinuclear oxo-bridged complexes have proved to be effective chemical nucleases [8, 9].

*Corresponding author. Email: yansp@nankai.edu.cn

Journal of Coordination Chemistry
ISSN 0095-8972 print/ISSN 1029-0389 online © 2009 Taylor & Francis
DOI: 10.1080/00958970802483632

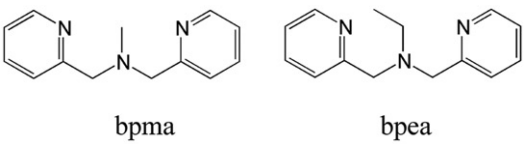

Scheme 1. The scheme of bpea and bpma.

For example, Que [8] synthesized a binuclear Fe(III) complex, $[Fe_2L(OH)(NO_3)_4]$ (HPTB = *N*, *N*, *N*′, *N*′-tetrakis(2-benzimidazolylmethyl)-2-hydroxyl-1,3-diaminopropane), which, in concert with H_2O_2, O_2 and reductant, effects double-strand cleavage of supercoiled pBR322 DNA by a hydrolytic mechanism. It does so efficiently at room temperature and may be useful as an artificial restriction enzyme. Recently, Chen *et al.* [9] designed a ligand in which a DNA intercalator (acridine) is linked to a binuclear ligand, and synthesized its diferric complex as a hydrolytic cleaving agent of DNA.

In this article, we selected classical tridentate nitrogen donor ligands bpa-R (bpa-R = alkyl substituted *bis*(2-pyridylmethyl)amino) [10] (scheme 1) and obtained a diiron(III) complex. A variety of transition metal complexes with bpa-R ligands have been reported [11–21]. Iron(III) centers linked by a bridging oxygen atom and two carboxylate bridges are well established in the structure of hemerythrin, a marine invertebrate respiratory protein, in its various forms [22–24]. In the last decades, many examples of complexes containing (μ-oxo)*bis*(μ-carboxylato)diiron(III) core have been widely studied utilizing a variety of facially capping tridentate nitrogen donor ligands [25–27], but studies on iron(III) complexes with bpa-R ligands are limited. Herein, the synthesis, structure, magnetism and DNA cleavage properties of a new diiron(III) complex $\{[Fe_2(bpma)(bpea)(\mu\text{-}CH_3COO)_2\,\mu\text{-}O)]\cdot(ClO_4)_2\cdot 0.5CH_3OH\}$ (**1**) are presented.

2. Experimental

2.1. *Materials and instrumentation*

The bpma and bpea were prepared following literature methods [28, 29]. Ethidium bromide (EB), calf thymus DNA (ct-DNA), and pBR322 DNA were from Sigma. Tris-HCl buffer solution was prepared using deionized sonicated triply distilled water. Unless stated, all other reagents used in this research were obtained from commercial sources and used without further purification. Solvents were purified by standard procedures.

Elemental analyses for C, H, and N were obtained on a Perkin–Elmer analyzer model 240. Infrared spectroscopy on KBr pellets was performed on a Bruker Vector 22 FT–IR spectrophotometer from 4000–400 cm^{-1}. Electronic spectra were measured on a JASCO V−570 spectrophotometer. The fluorescence spectral data were obtained on a MPF−4 fluorescence spectrophotometer. Magnetic susceptibilities on crystal samples were measured with a Quantum Design MPMS SQUID magnetometer with a continuous-flow helium cryostat in the temperature at 4–300 K. The applied

magnetic field was 0.2 T. Diamagnetic correction was made with Pascal's constants for all the constituent atoms. The Gel Imaging and documentation DigiDoc-It System were assessed using Labworks Imaging and Analysis Software (UVI, England).

2.2. *Preparation of complex*

2.2.1. $[Fe_2(bpma)(bpea)(\mu\text{-}CH_3COO)_2\,\mu\text{-}O)]\cdot(ClO_4)_2\cdot 0.5CH_3OH$ (1). To a methanolic solution (10 mL) of $Fe(ClO_4)_3\cdot 9H_2O$ (1 mmol) was added dropwise an acetonitrile solution (5 mL) of bpma (0.5 mmol) and bpea (0.5 mmol) with stirring. The black-green solution was stirred for 10 min at room temperature and added dropwise to HOAc/NaOAc (2 mL) buffer solution. The mixture was refluxed for 4 h in the presence of air, cooled and filtered. Deep blue-green block crystals of **1** suitable for X-ray structure analysis were obtained by slow evaporation of the filtrate, collected by filtration, washed with diethyl ether and dried in air. (Yield: ~37% based on the iron salts.) Anal. Calcd for $C_{31.50}H_{40}Cl_2Fe_2N_6O_{13.50}$ (**1**): C, 41.94; H, 4.44; N, 9.32%. Found: C, 42.17; H, 4.19; N, 9.11%.

The complex showed good solubility in water, high solubility in methanol and ethanol, dimethylformamide (DMF), and dimethyl sulfoxide (DMSO).

2.3. *X-ray crystallography*

Suitable single crystal with approximate dimensions of $0.36\times 0.25\times 0.19\,mm^3$ was used for X-ray diffraction analyses by mounting on the tip of a glass fiber in air. Data were collected on a Bruker Smart-1000 CCD diffractometer with Mo-Kα ($\lambda = 0.71073$ Å) at 293(2) K. The structure was solved by the direct method using SHELXS-97 [30] and subsequent Fourier difference techniques, and refined anisotropically by full matrix least-squares on F^2 using SHELXL-97 [31]. All nonhydrogen atoms were refined anisotropically and all hydrogens were located in the Fourier difference maps. Further crystallographic data and experimental details for structural analysis are summarized in table 1. Crystallographic data for the structure reported in this article have been deposited with the Cambridge Crystallographic Data Centre as supplementary publication No. CCDC-628650.

2.4. *DNA-binding and cleavage experiments*

The DNA-binding experiments were performed at room temperature. The solution of ct-DNA gave a ratio of UV absorbance at 260 nm and 280 nm, A_{260}/A_{280}, of 1.86, indicating that the DNA was sufficiently free of protein [32]. The ct-DNA stock solutions were prepared in 5 mM Tris-HCl/NaCl buffer, pH = 7.2 (stored at 4°C and used within 4 days after their preparation). The concentration of ct-DNA was determined from its absorption intensity at 260 nm with a molar extinction coefficient of $6600\,M^{-1}\,cm^{-1}$ [33].

UV–Visible absorption spectroscopy experiments were conducted by adding ct-DNA solution to **1** (5 μM) at different concentrations (0–160 μM). By fluorescence spectra, the relative binding of **1** to ct-DNA was studied with an EB-bound ct-DNA solution.

Table 1. Crystal data and structure refinement for **1**.

Complex	**1**
Empirical formula	$C_{31.50}H_{40}Cl_2Fe_2N_6O_{13.50}$
Formula weight	901.30
Crystal system	Monoclinic
Space group	$P2_1/c$
Unit cell dimensions	
	$a = 10.9434(12)$ Å
	$b = 23.118(3)$ Å
	$c = 15.8721(18)$ Å
	$\beta = 92.736(2)^\circ$
Z	4
$D_{Calcd.}$ (mg m^{-3})	1.493
Absorption coefficient (mm^{-1})	0.925
$F(000)$	1860
Crystal size (mm^3)	$0.36 \times 0.25 \times 0.19$
Limiting indices	$-13 \le h \le 12, -27 \le k \le 18, -18 \le l \le 17$
Reflections collected	21287
Independent reflections	7077 [$R_{int} = 0.0619$]
Data/restraints/parameters	7077/0/505
Goodness-of-fit on F^2	1.022
Final R indices [$I > 2\sigma(I)$]	$R_1 = 0.0764$, $wR_2 = 0.2067$
R indices (all data)	$R_1 = 0.1223$, $wR_2 = 0.2404$

The excitation wavelength was fixed at 510 nm and the emission range was adjusted before measurements. Fluorescence intensities at 602 nm were measured at different complex concentrations [34].

Cleavage of supercoiled pBR322 DNA by the complex was studied by agarose gel electrophoresis. The reaction was carried out following a literature method [35]. Bands were observed by UV light and photographed. The resolved bands were visualized by EB staining and were then quantified. A correction factor of 1.22 was utilized to account for the decreased ability of EB to intercalate into Form I DNA compared with Form II [36].

3. Results and discussion

3.1. *IR spectrum*

In the infrared spectra of **1**, ν_{as} (COO) and ν_s (COO) are 1552 and 1454 cm^{-1}, respectively, with the difference between them of 98 cm^{-1}, significantly lower than that of free carboxylate, indicating chelating carboxylate in **1** [37]. A strong band at 1087 cm^{-1} is assigned to $\nu(ClO_4^-)$.

3.2. *Description of the crystal structure of (1)*

The structure of **1** consists of $[Fe_2(bpma)(bpea)(\mu\text{-}CH_3COO)_2\,\mu\text{-}O)]^{2+}$, ClO_4^- anions and solvate CH_3OH molecules. The labeled diagram of the cation is shown in figure 1 and selected bond lengths and angles are listed in table 2. The geometry around Fe1

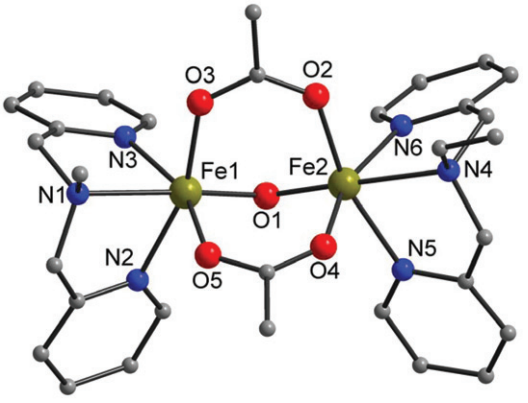

Figure 1. The labeled scheme of the binuclear unit of **1**; hydrogens, ClO_4^- and H_2O are omitted for clarity.

Table 2. Selected bond lengths (Å) and angles (°) for **1**.

Fe(1)–O(1)	1.795(4)	Fe(2)–O(1)	1.798(4)
Fe(1)–O(5)	1.998(5)	Fe(2)–O(4)	2.007(5)
Fe(1)–O(3)	2.023(5)	Fe(2)–O(2)	2.028(5)
Fe(1)–N(2)	2.143(6)	Fe(2)–N(6)	2.139(5)
Fe(1)–N(3)	2.153(5)	Fe(2)–N(5)	2.140(5)
Fe(1)–N(1)	2.263(6)	Fe(2)–N(4)	2.266(5)
Fe(1)– Fe(2)	3.064(1)		
O(1)–Fe(1)–O(5)	99.70(2)	O(1)–Fe(2)–O(4)	99.9(2)
O(1)–Fe(1)–O(3)	99.20(2)	O(1)–Fe(2)–O(2)	97.74(2)
O(5)–Fe(1)–O(3)	95.88(2)	O(4)–Fe(2)–O(2)	94.2(2)
O(1)–Fe(1)–N(2)	97.2(2)	O(1)–Fe(2)–N(6)	97.55(2)
O(5)–Fe(1)–N(2)	87.5(2)	O(4)–Fe(2)–N(6)	160.7(2)
O(3)–Fe(1)–N(2)	162.4(2)	O(2)–Fe(2)–N(6)	91.43(2)
O(1)–Fe(1)–N(3)	98.79(2)	O(1)–Fe(2)–N(5)	98.6(2)
O(5)–Fe(1)–N(3)	159.6(2)	O(4)–Fe(2)–N(5)	86.0(2)
O(3)–Fe(1)–N(3)	89.62(2)	O(2)–Fe(2)–N(5)	163.4(2)
N(2)–Fe(1)–N(3)	81.7(2)	N(6)–Fe(2)–N(5)	83.37(2)
O(1)–Fe(1)–N(1)	173.2(2)	O(1)–Fe(2)–N(4)	174.33(2)
O(5)–Fe(1)–N(1)	83.34(2)	O(4)–Fe(2)–N(4)	84.2(2)
O(3)–Fe(1)–N(1)	86.4(2)	O(2)–Fe(2)–N(4)	85.8(2)
N(2)–Fe(1)–N(1)	76.8(2)	N(6)–Fe(2)–N(4)	77.9(2)
N(3)–Fe(1)–N(1)	77.4(2)	N(5)–Fe(2)–N(4)	77.7(2)
Fe(1)–O(1)–Fe(2)	117.0(2)		

is a distorted octahedron, coordinated to three nitrogens of bpma (N1, N2, N3), two oxygens of bridging OAc^- groups (O3, O5) and the bridging oxygen (O1). The geometry around Fe2 is also a distorted octahedron. Fe2 iron is coordinated to three nitrogens of bpea (N4, N5, N6), two oxygens of the bridging OAc^- (O2, O4) and the bridging oxygen (O1). The structure consisting of (μ-oxo)-di-(μ-carboxylato) unit gives a Fe···Fe distance of 3.064 Å. The Fe-μ-O bond lengths (1.795/1.798 Å, table 2) are characteristic of the Fe(III)–O bridge, similar to those of Fe(III)-oxo bridge distances (<1.8 Å) [38, 39] and significantly smaller than the Fe(III)–OH bridge distance (1.97 Å) [40]. The Fe–O–Fe angle is 117.0° and the Fe1–$N_{average}$ and Fe2–$N_{average}$ distances are 2.186 and 2.182 Å, respectively.

3.3. *Magnetic properties*

Complex **1** was studied by magnetic susceptibility measurements from 4 to 300 K. The effective magnetic moment (μ_{eff}) and the molar magnetic susceptibilities (χ_M) *versus* T are plotted in figure 2. The μ_{eff} value per binuclear complex in **1** varies gradually from 2.39 B.M. at 300 K, which is much lower than the spin-only value of two high-spin Fe(III) atoms (8.37 B.M.), decreasing to 0.15 B.M. at 4 K. The behavior indicates strong intramolecular antiferromagnetic coupling of the high-spin irons, tending to a diamagnetic ($S=0$) ground state. The small increase in the magnetic susceptibility observed at low temperatures is due to a trace of monomeric impurity, which is a feature of complexes possessing antiferromagnetic interactions between the metal centers [41]. In this case, the molar paramagnetic susceptibility data fit an expression [42], which is based on the general isotropic exchange Hamiltonian, $\hat{H} = -2J\hat{S}_1 \cdot \hat{S}_2$, with J = magnetic exchange coupling constant and $S_1 = S_2 = 5/2$:

$$\chi_M = \frac{(1-\rho)Ng^2\beta^2(A/B)}{kT} + 4.375\rho/T + TIP$$

$$A = 2\exp(2x) + 10\exp(6x) + 28\exp(12x) + 60\exp(20x) + 110\exp(30x)$$

$$B = 1 + 3\exp(2x) + 5\exp(6x) + 7\exp(12x) + 9\exp(20x) + 11\exp(30x)$$

$$x = J/kT$$

The parameters obtained on fitting of the data were $g = 2.04$, $J = -121.0\,cm^{-1}$, $\rho = 0.14\%$ and the agreement factor defined by $R = \sum(\chi_{obsd} - \chi_{calcd})^2/\sum\chi_{obsd}{}^2$ is equal to 7.04×10^{-4}. The value of J demonstrates strong intramolecular antiferromagnetic coupling of the high-spin Fe(III) atoms, in good agreement with literature values observed for other (μ-oxo)*bis*(μ-carboxylato)-diiron(III) compounds, were found to be between -110 and $-140\,cm^{-1}$ [43].

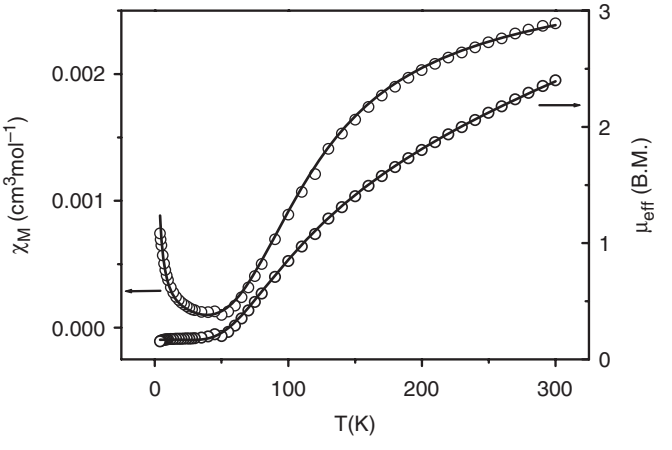

Figure 2. Plots of χ_M and μ_{eff} *vs.* T of **1**; Solid lines represent the best theoretical fits.

3.4. *DNA-binding and cleavage activity*

DNA binding is the critical step for DNA cleavage in most cases; therefore, the binding ability of the title complex with ct-DNA is characterized by measuring its effect on UV and fluorescence spectra of DNA.

3.5. *UV–Visible absorption spectroscopy*

The potential binding ability of **1** to ct-DNA was studied by UV spectroscopy. The interaction with ct-DNA was performed by following the intensity changes of the intraligand π–π^* transition band, as shown in figure 3. Upon addition of ct-DNA ($0-1.6\times10^{-4}$ M) to aqueous solution of **1** (5×10^{-6} M), both π–π^* transition bands exhibit significant hypochromism and a slight red shift in the UV spectra, similar to other dinuclear iron(III) complexes interacting with DNA [44]. The hypochromism reached as high as 27.2% at 231 nm with 3 nm red shift. The corresponding π–π^* band at 259 nm exhibited hypochromism about 36.1% and a bathochromic shift of 10 nm under similar experimental conditions. Complex bound to DNA through stacking interaction of the planar aromatic rings of the ligand with the base pairs of DNA usually result in hypochromism and red shift of ligand- and charge-transfer bands [45]. The intrinsic binding constant (K_b) for **1** to ct-DNA was calculated to be 5.18×10^3 (or $1.74\times10^3\,M^{-1}$) using the equation [46]: $[DNA]/(\varepsilon_A-\varepsilon_F)=[DNA]/(\varepsilon_B-\varepsilon_F)+1/K_b(\varepsilon_B-\varepsilon_F)$, here $\varepsilon_A, \varepsilon_F$, and ε_B correspond to A_{obsd}/[complex], the extinction coefficient for the free complex, and the extinction coefficient for the complex in the fully bound form, respectively. The value is much lower than those reported for classical intercalators (e.g., EB–DNA, $\sim10^5\,M^{-1}$) [47], indicating the affinity of **1** for DNA is moderate showing that intercalative binding is likely. Fe(III) and bpa alone did not show any sign of binding to ct-DNA in the UV-vis spectra under the same conditions.

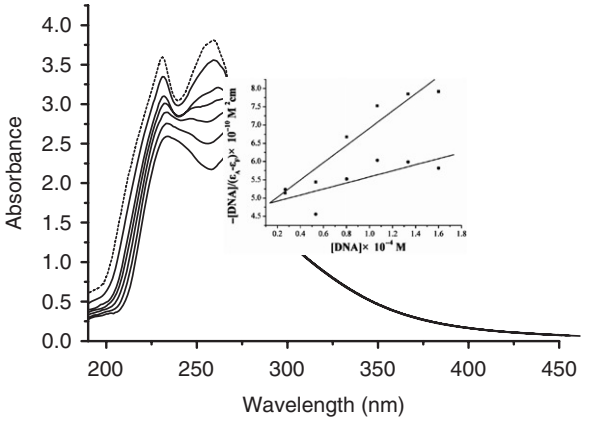

Figure 3. Absorption spectra of **1** (5×10^{-6} M) in the absence (dashed line) and presence (solid lines) of increasing amounts of ct-DNA (0–1.6×10^{-4} M) at room temperature in Tris-HCl/NaCl buffer (pH = 7.2).

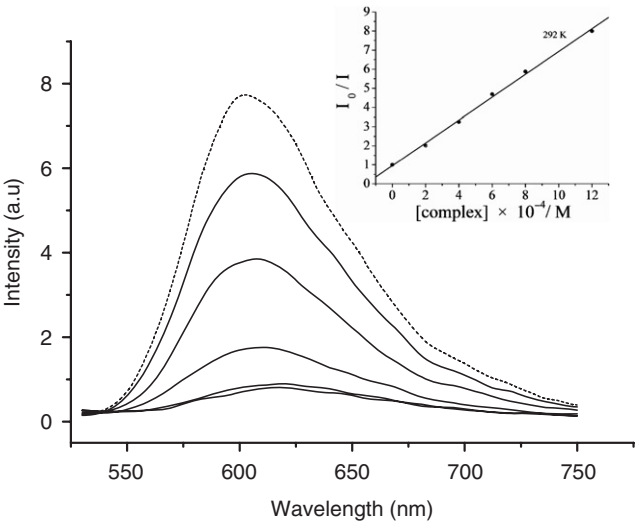

Figure 4. Emission spectra of EB–ct-DNA in the absence (dashed line) and presence (solid lines) of **1** at 292 K.

3.6. *Luminescence studies*

Figure 4 displays the fluorescence emission spectra of the EB–DNA system upon addition of the complex. As the title complex is nonemissive, relative binding studies with EB–ct-DNA were carried out to further explore the modes assessed from the above UV studies. EB emits intense fluorescence in the presence of DNA due to strong intercalation between adjacent DNA base pairs. It was previously reported that enhanced fluorescence could be quenched by the addition of another molecule. The relative binding propensity of the complex to ct-DNA was determined from comparison of the slopes of the lines in the fluorescence intensity *versus* complex concentration plot [48]. Such a plot of apparent binding suggests that the complex displaces DNA-bound EB and binds to DNA at the intercalation sites with almost the same affinity and the interaction of the complex with DNA is moderate. The apparent binding constants (K_{app}) at room temperature can be calculated from the experimental data by using the reported method [35]. The value obtained for **1** is $2.186 \times 10^5\,M^{-1}$, which is less than the binding constant of classical intercalators and metallointercalators ($10^7\,M^{-1}$) [49].

Many properties of metal complexes such as size, charge, shape, etc., could influence the binding mode. Taking the above UV–Vis and fluorescence spectra data together, a classical intercalation binding to DNA appears unlikely for **1**. The planar rigid groups of the ligands could intercalate to the small groove of DNA, giving moderate intercalation.

3.7. *DNA-cleavage activity*

The DNA cleavage activity of **1** has been studied under similar physiological pH and temperature by gel electrophoresis using supercoiled pBR322 plasmid DNA as the substrate. As shown in figure 5, with increase of the complex concentration, the

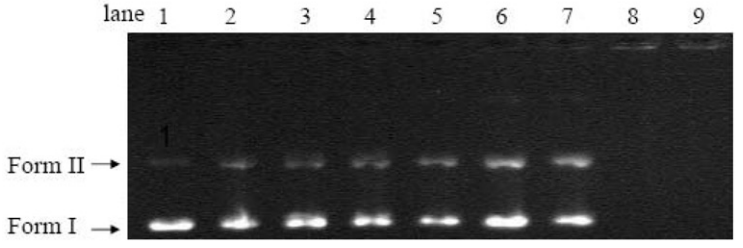

Figure 5. Gel electrophoresis diagrams showing the cleavage of pBR322 DNA at different complex concentrations in Tris-HCl/NaCl buffer (pH 6.0) and 37°C. Lane 1, DNA control (0.5 h); Lanes 2–8: DNA + complex **1** (0.011, 0.044, 0.088, 0.132, 0.176, 0.22, 0.242 mM) (0.5 h), respectively.

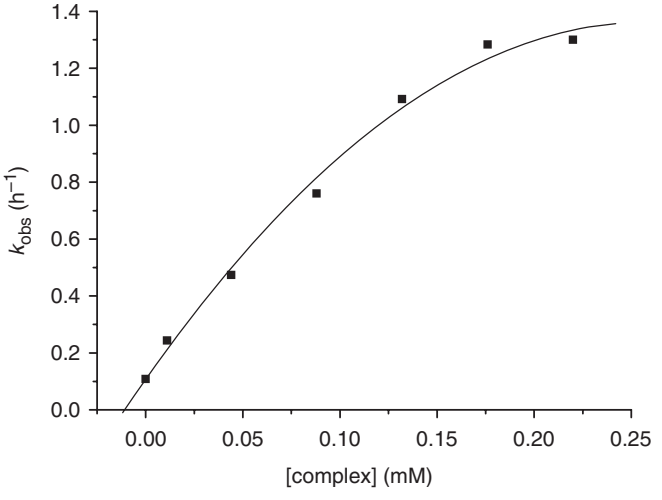

Figure 6. The plot of k_{obs} *vs.* [complex].

intensity of the circular supercoiled DNA (Form I) band decreases, while that of nicked (Form II) bands increase (lane 2–7) in the absence of any activating agents. When the complex concentration was 0.242 mM (line 8), Form II disappeared and completely turned into small fragments. The structure of the ligand plays an important role in the DNA-binding mode [50]. Ligands with polyamine groups show better binding abilities because they may bind with DNA through electrostatics and hydrogen bonding interactions [51]. DNA cleavage ability after combining to the metal ions was promoted [52]. Bridged-oxo on the linkage also likely assists the cleavage process.

Saturation kinetics of DNA cleavage were studied at various concentrations of complex. Since cuts of Form I are exclusively responsible for generating Form II, one can assume that the plot for the appearance of Form II as well as the disappearance of Form I follow pseudo-first-order kinetic profiles and fit well to a single-exponential decay curve. The rate of reaction at complex concentration of 0.132 mM was to be 1.092 h^{-1} for increase of Form II. Similarly, the rate of reaction for DNA in the presence of 0.011–0.22 mM **1** was obtained (figure 6). The kinetic measurements showed that rate constants rapidly increase at beginning, then saturate with increasing DNA concentration, normal saturation behavior, fulfilling the Michaelis–Menten

kinetics equation. Based on the plots of k_{obs} *versus* concentrations of complex, the pseudo-Michaelis–Menten kinetic parameters $k_{cat} = 4.47\,h^{-1}$ and $K_m = 7.15 \times 10^{-5}\,M$ are obtained for **1**. Examples of Fe(III)-based artificial nucleases reported to date are scarce [44].

Acknowledgements

This work was supported financially by the National Science Foundation of China (No. 20331020, 20571056 and 20771063), the Education Science Foundation of Tianjin City (No. 20070606) and the PhD Foundation of Tianjin Normal University (No. 52LX28).

References

[1] P.A.N. Reddy, B.K. Santra, M. Nethaji, A.R. Chakravarty. *J. Inorg. Biochem.*, **98**, 377 (2004).
[2] A. Neves, H. Terenzi, R. Hörner, A. Horn Jr, B. Szpoganicz, J. Sugai. *Inorg. Chem. Commun.*, **4**, 388 (2001).
[3] K. Yamaguchi, F. Akagi, S. Fujinami, M. Suzuki, M. Shionoya, S. Suzuki. *Chem. Commun.*, 375 (2001).
[4] L.M. Rossi, A. Neves, R. Hörner, H. Terenzi, B. Szpoganicz, J. Sugai. *Inorg. Chim. Acta*, **337**, 366 (2002).
[5] K. Yamada, Y. Takahashi, H. Yamamura, S. Araki, K. Saito, M. Kawai. *Chem. Commun.*, 1315 (2000).
[6] Y. Gultneh, A.R. Khan, D. Blaise, S. Chaudhry, B. Ahvazi, B.B. Marvey, R.J. Butcher. *J. Inorg. Biochem.*, **75**, 7 (1999).
[7] L. Zhu, O. dos Santos, C.W. Koo, M. Rybstein, L. Pape, J.W. Canary. *Inorg. Chem.*, **42**, 7912 (2003).
[8] L.H. Schnaith, R.S. Hanson, L. Que Jr. *Proc. Natl. Acad. Sci.*, **91**, 569 (1994).
[9] X.Q. Chen, X.J. Peng, J.Y. Wang, Y. Wang, S. Wu, L.Z. Zhang, T. Wu, Y.K. Wu. *Eur. J. Inorg. Chem.*, **34**, 5400 (2007).
[10] J.K. Romary, J.D. Barger, J.E. Bunds. *Inorg. Chem.*, **7**, 1142 (1968).
[11] J. Mukherjee, V. Balamurugan, R. Gupta, R. Mukherjee. *Dalton Trans.*, 3686 (2003).
[12] A. Hazell, C.J. Mckenzie, L.P. Nielsen. *Polyhedron*, **19**, 1333 (2000).
[13] C. Baffert, I. Romero, J. Pécaut, A. Llobet, A. Deronzier, M.N. Collomb. *Inorg. Chim. Acta*, **357**, 3430 (2004).
[14] M. Ito, Y. Takita, K. Sakai, T. Tubomura. *Chem. Lett.*, 1185 (1998).
[15] S.K. Mandal, W.H. Armstrong. *Inorg. Chim. Acta*, **229**, 261 (1995).
[16] D.R. van Staveren, E. Bothe, T. Weyhermůller, N. Metzler-Nolte. *Eur. J. Inorg. Chem.*, **6**, 1518 (2002).
[17] M. Rodríguez, I. Romero, A. llobet, A. Deronzier, M. Biner, T. Parella, H. Stoeckli-Evans. *Inorg. Chem.*, **40**, 4150 (2001).
[18] I. Romero, L. Dubois, M.N. Collomb, A. Deronzier, J.M. Latour, J. Pécaut. *Inorg. Chem.*, **41**, 1795 (2002).
[19] C. Mantel, A.K. Hassan, J. Pécaut, A. Deronizier, M.N. Collomb, C. Duboc-Toia. *J. Am. Chem. Soc.*, **125**, 12337 (2003).
[20] C.E. Dubé, D.W. Wright, S. Pal, P.J. Bonitatebus Jr, W.H. Armstrong. *J. Am. Chem. Soc.*, **120**, 3704 (1998).
[21] S. Thewissen, M.D.M. Reijnders, J.M.M. Smits, B.de. Bruin. *Organometallics*, **24**, 5964 (2005).
[22] P.C. Wilkins, R.G. Wilkins. *Coord. Chem. Rev.*, **79**, 195 (1987).
[23] R.E. Stenkamp. *Chem. Rev.*, **94**, 715 (1994).
[24] J. Du Bois, T.J. Mizoguchi, S.J. Lippard. *Coord. Chem. Rev.*, **200–202**, 443 (2000).
[25] D.M. Kuriz Jr. *Chem. Rev.*, **90**, 585 (1990).
[26] S.J. Lippard. *Angew. Chem., Int. Ed. Engl.*, **27**, 344 (1988).
[27] L. Que Jr, A.E. True. *Prog. Inorg. Chem.*, **38**, 97 (1990).
[28] K.B. Jensen, C.J. Mckenzie, O. Simonsen, H. Toftlund, A. Hazell. *Inorg. Chim. Atca*, **257**, 163 (1997).
[29] S. Pal, M.K. Chan, W.H. Armstrong. *J. Am. Chem. Soc.*, **114**, 6398 (1992).
[30] G.M. Sheldrick. *SHELXS 97, Program for the Solution of Crystal Structures*, University of Gottingen, Gottingen (1997).

[31] G.M. Sheldrick. *SHELXL 97, Program for the Refinement of Crystal Structures*, University of Gottingen, Gottingen (1997).
[32] J. Marmur. *J. Mol. Biol.*, **3**, 208 (1961).
[33] M.E. Reichmann, S.A. Rice, C.A. Thomas, P. Doty. *J. Am. Chem. Soc.*, **76**, 3047 (1954).
[34] B.C. Baguley, M. Le Bret. *Biochemistry*, **23**, 937 (1984).
[35] J. Qian, W. Gu, H. Liu, F.X. Gao, L. Feng, S.P. Yan. *Dalton Trans.*, 1060 (2007).
[36] W.H. Armstrong, S.J. Lippard. *J. Am. Chem. Soc.*, **106**, 4632 (1984).
[37] R.P. Hertzberg, P.B. Dervan. *J. Am. Chem. Soc.*, **104**, 313 (1982).
[38] G.B. Deacon, R.J. Phillips. *Coord. Chem. Rev.*, **33**, 227 (1980).
[39] P.N. Turowski, W.H. Armstrong, S. Liu, S.N. Brown, S.J. Lippard. *Inorg. Chem.*, **33**, 636 (1994).
[40] M.A. Alam, M. Nethaji, M. Ray. *Inorg. Chem.*, **44**, 1302 (2005).
[41] P.E. Kruger, B. Moubaraki, G.D. Fallon, K.S. Murray. *J. Chem. Soc., Dalton Trans.*, 713 (2000).
[42] C.J. O'Connor. *Prog. Inorg. Chem.*, **29**, 203 (1990).
[43] K.B. Jensen, C.J. McKenzie, O. Simonsen, H. Toftlund, A. Hazell. *Inorg. Chim. Acta*, **257**, 163 (1997).
[44] F.B.A.E. Amrani, L. Perelló, J.A. Real, M.G. Alvarez, G. Alzuet, J. Borrás, J.M. Bernardo. *J. Inorg. Biochem.*, **100**, 1208 (2006).
[45] V.A. Bloomfield, D.M. Crothers Jr, I. Tinocco. *Physical Chemistry of Nucleic Acids*, p. 432, Harper & Row, New York (1974).
[46] A. Wolfe, G.H. Shimer, T. Meehan. *Biochemistry*, **26**, 6392 (1987).
[47] J.B. Le Pecq, C. Paoletti. *J. Mol. Biol.*, **27**, 87 (1967).
[48] J. Bermadou, G. Pratviel, F. Bennis, M. Girardet, B. Meunier. *Biochemistry*, **28**, 7268 (1989).
[49] M. Cory, D.D. Mckee, J. Kagan, D.W. Henry, J.A. Miller. *J. Am. Chem. Soc.*, **107**, 2528 (1985).
[50] Y.M. Zhao, J.H. Zhu, W.J. He, Z. Yang, Y.G. Zhu, Y.Z. Li, J.F. Zhang, Z.J. Guo. *Chem. Eur. J.*, **12**, 6621 (2006).
[51] C. Tu, Y. Shao, N. Gan, Q. Xu, Z.J. Guo. *Inorg. Chem.*, **43**, 4761 (2004).
[52] M.C.B. Oliveira, M.S.R. Couto, P.C. Severino, T. Foppa, G.T.S. Martins, B. Szpoganicz, R.A. Peralta, A. Neves, H. Terenzi. *Polyhedron*, **24**, 495 (2005).